

See discussions, stats, and author profiles for this publication at: <https://www.researchgate.net/publication/26836395>

Climate change: The El Niño with a difference

Article in *Nature* · September 2009

DOI: 10.1038/461481a · Source: PubMed

CITATIONS

174

READS

520

2 authors:



Karumuri Ashok

University of Hyderabad

63 PUBLICATIONS 3,204 CITATIONS

[SEE PROFILE](#)



Toshio Yamagata

Japan Agency for Marine-Earth Science Tech...

349 PUBLICATIONS 16,867 CITATIONS

[SEE PROFILE](#)

Some of the authors of this publication are also working on these related projects:



Non-linearities of the ENSO flavors [View project](#)



Extreme Rainfall events, tropical ocean drivers, and background changes [View project](#)

All content following this page was uploaded by **Karumuri Ashok** on 29 March 2017.

The user has requested enhancement of the downloaded file. All in-text references [underlined in blue](#) are added to the original document and are linked to publications on ResearchGate, letting you access and read them immediately.

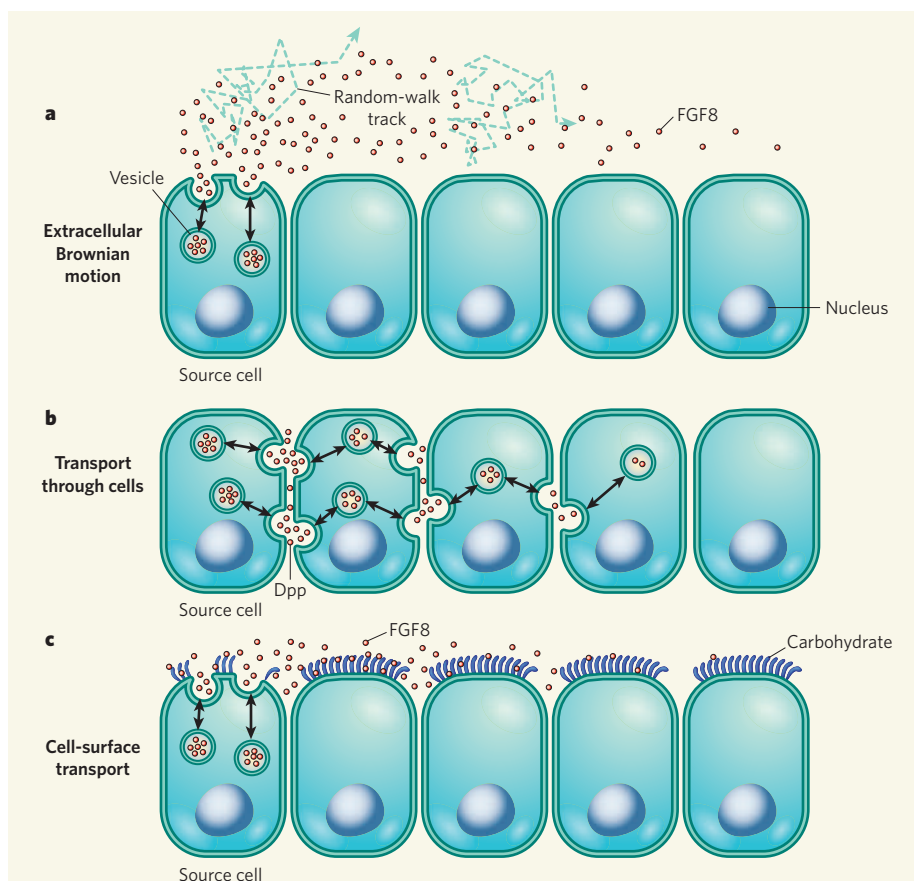


Figure 1 | Models of morphogen dispersal. Source cells harbour vesicles filled with morphogen molecules (red), which fuse with the cell membrane and release their contents. **a**, Yu *et al.*² propose that Brownian motion of molecules in the extracellular space leads to dispersal of the FGF8 morphogen. Two tracks of random walk by single FGF8 molecules are shown. **b**, Kicheva and colleagues⁵ suggest that repeated release and uptake by cells (transcytosis) leads to dispersal of the morphogen Dpp in the fly wing. **c**, A few slowly diffusing FGF8 molecules are associated with carbohydrates at the cell surface³. This cell-surface pool may contribute to long-range dispersal of FGF8.

of FGF8 increases the distance range of the gradient. In this scenario, the sink is not only at one end of the tissue, but is formed by all the target cells that contribute to morphogen removal and gradient formation.

In Yu and colleagues' model², the transport of FGF8 is driven by Brownian motion through extracellular space, as Francis Crick proposed (Fig. 1a). But this might not be the only way of establishing morphogen gradients. In their studies of the morphogen Decapentaplegic (Dpp) protein in *Drosophila*, Kicheva *et al.*⁵ photobleached a large region of the developing wing of the fly and measured the time it took for fluorescently labelled Dpp molecules to re-enter the bleached region. Their result — an effective diffusion coefficient of only $\sim 0.1 \mu\text{m}^2 \text{s}^{-1}$ — means that the typical time taken for Dpp to travel a certain distance would be nearly three orders of magnitude longer than for FGF8. One explanation for this is that the Dpp gradient might be generated by transport through cells⁵ (Fig. 1b). In this case, the repeated cellular uptake and release of Dpp (transcytosis) would lead to an effective diffusion coefficient that is much lower than that of the freely diffusing FGF8.

Why are the results for FGF8 and Dpp so different? The simplest explanation is that these systems really are dissimilar. After all, a fly wing is not a zebrafish embryo, and the principles responsible for establishing

morphogen gradients in these two structures might not be the same.

It is important to keep in mind, however, that different methods were used to measure morphogen transport in the two studies. The FCS experiments provide data on the motion of FGF8 through a volume of $\sim 0.1 \mu\text{m}^3$, whereas the photobleaching experiments measure the recovery of Dpp into a volume of $\sim 10^4 \mu\text{m}^3$, a difference of five orders of magnitude. It might be that the small-scale motion measured by FCS and the large-scale motion observed by photobleaching occur by different mechanisms. If that were the case, FGF8 and Dpp might be dispersed in a similar fashion, and the two studies may have simply probed different aspects of morphogen motion. In this context, it is interesting to note that Yu *et al.*² identified a second, minor fraction of FGF8 that has a 10-fold lower diffusion coefficient. This fraction of FGF8 seems to be associated with carbohydrates located at the surface of cells. The role of this pool of FGF8 is unclear, but it might contribute to the spread of FGF8 along the cell surface (Fig. 1c).

The studies of FGF8² and Dpp⁵ have revealed unexpected complexity of morphogen dispersal. They raise the question of what the biophysical properties of other signalling molecules are during development. Do they function like FGF8 or do they resemble Dpp? The further application of quantitative approaches to other systems and organisms will hopefully address these questions.

Alexander F. Schier and Daniel Needleman are in the Department of Molecular and Cellular Biology, Harvard University, Cambridge, Massachusetts 0218, USA.
e-mail: schier@mcb.harvard.edu

1. Gurdon, J. B. & Bourillot, P. Y. *Nature* **413**, 797–803 (2001).
2. Yu, S. R. *et al.* *Nature* **461**, 533–536 (2009).
3. Crick, F. *Nature* **225**, 420–422 (1970).
4. Magde, D., Elson, E. & Webb, W. *Phys. Rev. Lett.* **29**, 705–708 (1972).
5. Kicheva, A. *et al.* *Science* **315**, 521–525 (2007).

CLIMATE CHANGE

The El Niño with a difference

Karumuri Ashok and Toshio Yamagata

Patterns of sea-surface warming and cooling in the tropical Pacific seem to be changing, as do the associated atmospheric effects. Increased global warming is implicated in these shifts in El Niño phenomena.

Through the El Niño events^{1,2} that occur every 3–8 years or so, the state of the tropical Pacific Ocean and overlying atmosphere has global effects on climate — sometimes with devastating effects, for example on agriculture in India. El Niños are defined by warmer than normal sea surface temperatures in the eastern tropical Pacific, and are associated with

anomalous atmospheric circulation patterns known as the Southern Oscillation. These coupled phenomena, together called ENSO, have been the subject of research since the late nineteenth century. They remain a matter of intense interest today, not least because of a puzzling shift in behaviour over recent years. That shift, and its possible causes, is the

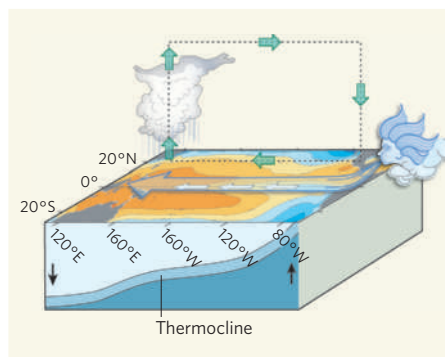


Figure 1 | Normal conditions in the tropical Pacific. Warm surface water and air are pushed to the west by prevailing winds. A consequence is upwelling of cold water on the eastern side, and a shallow thermocline (a subsurface boundary that marks a sharp contrast between warm upper waters and colder deeper waters). Opposite oceanographic conditions prevail on the western side. In the atmosphere, the west is warmer and wetter. Here and in Figure 2, redder colours denote warmer waters, bluer colours denote cooler waters.

subject of the paper by Yeh *et al.*³ that appears on page 511 of this issue.

Normal conditions in the tropical Pacific are shown in Figure 1, and El Niño conditions in Figure 2a. But since the late 1970s, events with increased sea surface temperatures (SSTs) in the central Pacific, sandwiched by anomalous cooling in the east and west, have been observed⁴. These are not like the conventional El Niño: rather, the maximum SST anomaly persists in the central Pacific from the boreal summer through to the winter, modifying the atmospheric circulation and resulting in distinctly different global impacts^{4–10}. This phenomenon has been viewed as a different ‘flavour’ of El Niño⁵, with warming around the Date Line rather than farther east⁶. In other studies^{4,9,10} it has been classified as a new type of tropical Pacific phenomenon, and named El Niño Modoki, or Pseudo El Niño, to stress the differences from the conventional El Niño. Other names, such as Central El Niño¹¹ and Warm Pool El Niño¹², have been proposed. But all of these refer to the same basic phenomenon, shown in Figure 2b, as viewed from slightly different standpoints.

What has caused this recent increased occurrence of the new-flavour of El Niño, with its distinct impact on the northern Pacific SST, compared with the normal form? Some analyses of observational data attribute it to consequences of the prominent global warming⁴ since the late 1970s — which include changes in the zonal tilt of the thermocline^{4,12}, the distinctive subsurface oceanic boundary between warmer and colder water, and weakened low-level easterly winds in the equatorial region. Yeh *et al.*³ have investigated these possibilities further by taking the data set of observed SSTs since the 1850s, and other climate data since the 1950s, and subjecting all this information to detailed analysis in computer models

of ocean–atmosphere behaviour.

Specifically, the authors compare the outcomes of the models used by the Program for Climate Model Diagnosis and Intercomparison (PCMDI). The model outcomes derive from two types of simulation data run through 11 ocean–atmosphere climate models. The control run represents twentieth-century climate change with anthropogenic and natural forcing up to 2000. The other run is from 100 years of a climate-change simulation based on the so-called global-warming SRES A1B scenario, in which levels of carbon dioxide are maintained at about 700 parts per million.

Yeh *et al.* call the canonical El Niño the Eastern Pacific (EP) El Niño, and the new phenomenon the Central Pacific (CP) El Niño. To define the EP events, they use a well-known measure, the NINO3 index, which is SST anomalies averaged over the area 5° N–5° S, 150° W–90° W. To define the CP events, they use a combination of the NINO3 and NINO4 indices, the latter an average of SST anomalies over 5° N–5° S, 160° E–150° W. They analyse the results from the individual model simulations as well as those aggregated by a multi-model, multi-ensemble method, a technique that is applied in operational dynamical seasonal prediction.

Through standardized error analysis, Yeh

et al. find that, in 8 models out of the 11 considered, the occurrence ratio of the CP-El Niño to the EP-El Niño increases in the global-warming scenario as compared to the corresponding twentieth-century climate simulation. The ratio is significantly higher at 95% confidence level in the global-warming simulations of 4 models out of a subset of 6 with more accurate simulations of the currently observed occurrence ratio. Furthermore, the observed remote impacts on SSTs in the Northern Hemisphere are qualitatively evident in the aggregated atmospheric simulations from 9 models. We must take into account that almost all coupled models are biased in representing ocean–atmosphere climatology and the El Niño SST pattern, intensity and frequency. Nonetheless, all these findings support the hypotheses that the increasing frequency of a new type of El Niño — Modoki, CP-El Niño, call it what you will — is due to global warming, and that, as anthropogenic global warming intensifies, we may see more of these events at the expense of the conventional El Niño.

Much more investigation is needed of course. Only four of the models provide statistically significant support, and the coupled models in the PCMDI have flaws in the realistic simulation of basin-wide structure (see Fig. 4 of the authors’ Supplementary

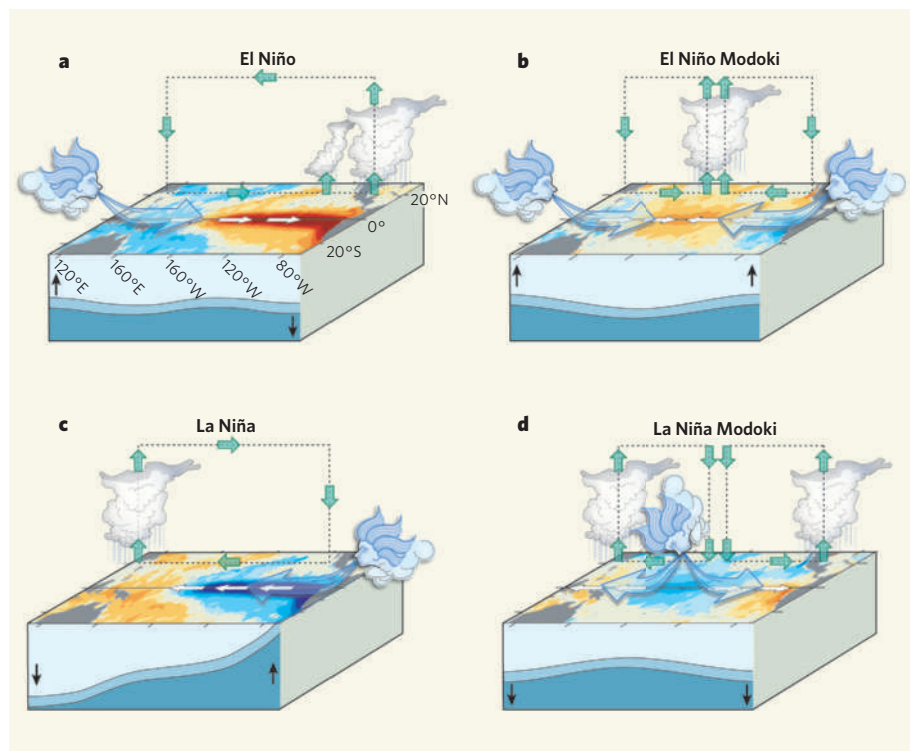


Figure 2 | Anomalous conditions in the tropical Pacific. **a**, An El Niño event is produced when the easterly winds weaken; sometimes, in the west, westerlies prevail. This condition is categorized by warmer than normal sea surface temperatures (SSTs) in the east of the ocean, and is associated with alterations in the thermocline and in the atmospheric circulation that make the east wetter and the west drier. **b**, An El Niño Modoki event is an anomalous condition of a distinctly different kind. The warmest SSTs occur in the central Pacific, flanked by colder waters to the east and west, and are associated with distinct patterns of atmospheric convection. **c**, **d**, The opposite (La Niña) phases of the El Niño and El Niño Modoki respectively. Yeh *et al.*³ argue that the increasing frequency of the Modoki condition is due to anthropogenic warming, and that these events in the central Pacific will occur more frequently if global warming increases.

Information³). Another hypothesis, that the modal shift in El Niño is just a manifestation of natural climate variability on decadal to centennial timescales, also needs to be examined, at least in model simulations. One such study¹³ indicates that both the frequency and the intensity of the ENSO change on multi-centennial timescales.

From the perspective of society's adaptation to climate change, predicting the El Niño Modoki is essential because of its distinctive global impacts on various timescales^{4–11,14,15}. However, our recent experience shows that the effectiveness of the current coupled models in predicting the ENSO Modoki index is low compared with their predictions of the conventional ENSO indices. Further improvement of methods for assimilating observed data into models, as well as improvement of seasonal

prediction models, is necessary. It is also worth examining whether the increasing frequency of the Modoki is related to the recent decadal shift in another ocean–atmosphere phenomenon, the Indian Ocean Dipole: over the past 50 years the SST of the Indian Ocean has increased by about 0.6 °C.

Karumuri Ashok is at the APEC Climate Center, 1463 U-dong, Haeundae-gu, Busan 612-020, Republic of Korea. Toshio Yamagata is at the Application Laboratory, JAMSTEC, 3173-25 Showa-machi, Kanazawa-ku, Yokohama 236-0001, Japan.
e-mails: ashok@apcc21.net (karumuriashok@hotmail.com); yamagata@jamstec.go.jp

1. Rasmusson, E. M. & Carpenter, T. H. *Mon. Weath. Rev.* **110**, 354–384 (1982).

2. Philander, S. G. H. *El Niño, La Niña, and the Southern Oscillation* (Academic, 1990).
3. Yeh, S.-W. *et al. Nature* **461**, 511–514 (2009).
4. Ashok, K., Behera, S. K., Rao, S. A., Weng, H. & Yamagata, T. *J. Geophys. Res.* **112**, doi:10.1029/2006JC003798 (2007).
5. Trenberth, K. E. & Stepaniak, D. P. *J. Clim.* **14**, 1697–1701 (2001).
6. Larkin, N. K. & Harrison, D. E. *Geophys. Res. Lett.* **32**, doi:10.1029/2005GL022738 (2005).
7. Kumar, K. K. *et al. Science* **314**, 115–119 (2006).
8. Wang, G. & Hendon, H. H. *J. Clim.* **20**, 4211–4226 (2007).
9. Weng, H., Ashok, K., Behera, S. K., Rao, S. A. & Yamagata, T. *Clim. Dynam.* **29**, doi:10.1007/s00382-008-0394-6 (2007).
10. Weng, H., Behera, S. K. & Yamagata, T. *Clim. Dynam.* **32**, doi:10.1007/s00382-008-0394-6 (2009).
11. Kao, H.-Y. & Yu, J.-Y. *J. Clim.* **22**, 615–632 (2009).
12. Kug, J.-S., Jin, F.-F. & An, S.-I. *J. Clim.* **22**, 1499–1515 (2009).
13. Wittenberg, A. T. *Geophys. Res. Lett.* **36**, doi:10.1029/2009GL038710 (2009).
14. Kim, H.-M., Webster, P. J. & Curry, J. A. *Science* **325**, 77–80 (2009).
15. Ashok, K., Tam, C.-Y. & Lee, W.-J. *Geophys. Res. Lett.* **36**, doi:10.1029/2009GL038847 (2009).

CHEMICAL BIOLOGY

Caught in the activation

Yi Liu

A crystal structure reveals how a protein kinase is activated by the binding of a small molecule at a pocket far from the catalytic site. This opens the door to the design of modulators of protein phosphorylation.

The protein functions that regulate cell behaviour are themselves tightly regulated by many different inputs. One of these is phosphorylation, the process in which a phosphate group from an ATP molecule is attached to a protein by a protein kinase enzyme¹. There is considerable interest in identifying small molecules that can modulate protein kinase activity, both as research tools and as potential human therapeutic agents. Indeed, eleven kinase inhibitors are already used as drugs for treating cancer, and several more are in clinical trials for the treatment of immune and inflammatory diseases².

Identifying protein kinase inhibitors is relatively easy — it's 'simply' a matter of finding molecules that prevent substrates from binding to the catalytic site of the enzyme. It has proved much more difficult to identify small molecules that activate these enzymes, but a few have been discovered, including those described in 2006 by Engel and colleagues³. Reporting in *Nature Chemical Biology*, the same group (Hindie *et al.*⁴) now disclose the crystal structure of the protein kinase PDK1 in a complex with one of these activators. This is the first crystal structure of a small-molecule activator bound to a protein kinase, and it provides a structural explanation of how this binding activates the enzyme.

A protein kinase catalytic domain consists of a small amino-terminal lobe and a large carboxy-terminal lobe (Fig. 1a). ATP binds in the cleft between the two lobes, whereupon its

terminal phosphate group can be transferred to the protein substrate also bound to the enzyme. Three regions in the ATP-binding site must be precisely positioned for efficient catalysis of the phosphate-transfer reaction: a loop rich in glycine amino acids (the Gly-rich loop); an α -helix

from the small lobe (known as the α -C-helix); and the 'activation' loop from the large lobe. To be activated, most protein kinases must first be phosphorylated in the activation loop⁵, but for full activation some also require a protein to bind to a site remote from the ATP site⁶. In PDK1, for example, a binding site known as the PIF-binding pocket in the small lobe recognizes a phosphorylated amino-acid sequence that activates the kinase⁷.

The authors' PDK1 activators³ bind at the PIF-binding pocket, thus offering the team a golden opportunity to investigate the molecular mechanism of kinase activation mediated by this site. By solving the crystal structure⁴ of a PDK1–activator complex, they found that activator binding causes a change in the conformation

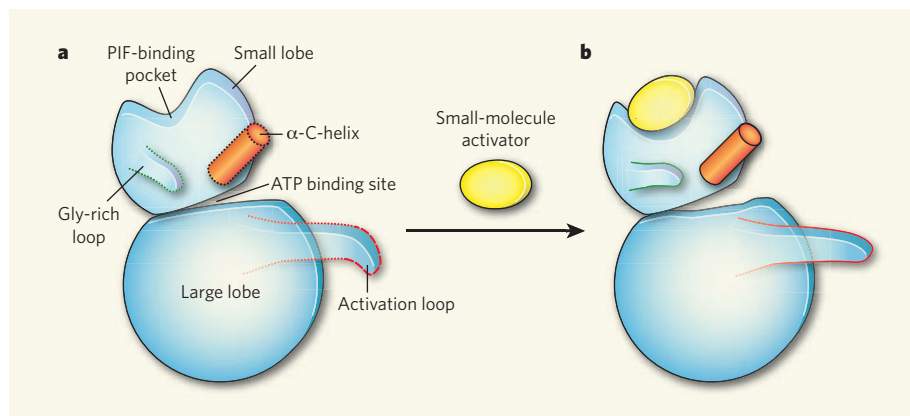


Figure 1 | Small-molecule activation of PDK1. The protein kinase enzyme PDK1 transfers phosphate groups from ATP to a protein substrate, and consists of a large and a small lobe. **a**, Three regions around the ATP-binding site of the enzyme are critical for PDK1 activity — a loop rich in the amino acid glycine (the Gly-rich loop), the α -C-helix and an activation loop. In the inactive state, these regions are flexible and in motion (indicated by dotted lines), and are not aligned for catalysis. Part of the activation loop is unstructured (dashed lines). **b**, Hindie *et al.*⁴ report the crystal structure of PDK1 in a complex with a small-molecule activator of the enzyme. The activator binds at a location known as the PIF-binding pocket, which is remote from the ATP-binding site. Activator binding induces local conformational changes around the PIF-binding pocket, which stabilize the structures of the nearby Gly-rich loop and α -C-helix, leading to conformational changes in these two regions. This stabilization acts as a signal to the disordered region of the activation loop, which adopts an ordered structure in response. Thus, binding of a small-molecule activator to the PIF-binding pocket orients the ATP-binding site into a conformation that is efficient for catalysing phosphate-transfer reactions.